University Library

MINERVA ACCESS

A gateway to Melbourne's research publications

Minerva Access is the Institutional Repository of The University of Melbourne

Author/s:
Allison-Logan, S;Fu, Q;Sun, Y;Liu, M;Xie, J;Tang, J;Qiao, GG

Title:
From UV to NIR: A Full-Spectrum Metal-Free Photocatalyst for Efficient Polymer Synthesis in Aqueous Conditions

Date:
2020-01-01

Citation:
Allison-Logan, S., Fu, Q., Sun, Y., Liu, M., Xie, J., Tang, J. & Qiao, G. G. (2020). From UV to NIR: A Full-Spectrum Metal-Free Photocatalyst for Efficient Polymer Synthesis in Aqueous Conditions. Angewandte Chemie, 132 (48), pp.21576-21580. https://doi.org/10.1002/ange.202007196.

Persistent Link:
https://hdl.handle.net/11343/275232

Check for updates

Author Manuscript

Title: From UV to NIR: A full spectrum metal-free photocatalyst for efficient polymer synthesis in aqueous conditions

Authors: Stephanie Allison-Logan; Qiang Fu, PhD; Yongkang Sun; Min Liu; Jijia Xie, PhD; Junwang Tang, PhD; Greg G. Qiao, PhD

This is the author manuscript accepted for publication. It has not been through the copyediting, typesetting, pagination and proofreading process, which may lead to differences between this version and the Version of Record.

To be cited as: 10.1002/ange.202007196

Link to VoR: https://doi.org/10.1002/ange.202007196

Professor Greg G. Qiao *FRACI C CHEM*
Direct Phone: +61 3 8344 8665
E-mail: gregghq@unimelb.edu.au

THE UNIVERSITY OF MELBOURNE

20 June 2020

To: Angewandte Chemie

Manuscript Title:

From UV to NIR: A full spectrum metal-free photocatalyst for efficient polymer synthesis in aqueous conditions

By Allison-Logan, S. et al.

Dear Dr. Horner,

We wish to thank the reviewers for taking the time to provide feedback. We thoroughly appreciate their recognition of our work and the relevant issues raised. Please find below the point-by-point reply to the comments (shown in red).

REVIEWER REPORT

EVALUATION:

Reviewer's Responses to Questions

1. Please rate the importance of the reported results

Reviewer #1: Highly important (top 20%)
Reviewer #2: Very important (top 5%)

---

2. Please rate the citation of previous publications

Reviewer #1: Appropriate
Reviewer #2: Appropriate

---

3. Please rate the length of the manuscript

Reviewer #1: Concise
Reviewer #2: Concise

---

4. Please rate the verification of hypotheses and conclusions by the presented data

Author Manuscript

This article is protected by copyright. All rights reserved

Reviewer #1: Minor inconsistencies
Reviewer #2: Fully consistent

---

5. Please indicate which other journal you consider more appropriate
Reviewer #1:
*----

Reviewer #2: (No Response)

COMMENTS TO AUTHOR:

Reviewer 1:
The manuscript "From UV to NIR: A full spectrum metal-free photocatalyst for efficient polymer synthesis in aqueous conditions" reports interesting results that deserve publication. Oxygen tolerant radical polymerization systems have received big interest. Interesting is the porphyrin that covers a broad spectral range with sufficient reactivity. The PC was designed as SA system showing interesting effects.

However, I have some questions:

1. Can authors provide results about block copolymerization? They mainly provided results obtained by chain extension.

Retention of the RAFT agent can be demonstrated through chain extension (pseudo-block) or block polymerizations. Although block polymers are of great interest, use of another water-soluble monomer would not provide more meaningful information for our system. The low dispersities, excellent agreement between theoretical and experimental results, and clear shift in polymer peak during chain extensions demonstrate the highly "living" nature of our system and that the vast majority of RAFT agent remains intact. This is further supported by the NMR data included as Figure S9 in response to Reviewer 1's comment 4.

2. What were the Mn of chain extension? Please add data.

Thank you for pointing out this oversight. Figure 2C has been modified as shown below to include the $M_{n\ GPC}$, dispersity, and conversion of the chain extension polymers.

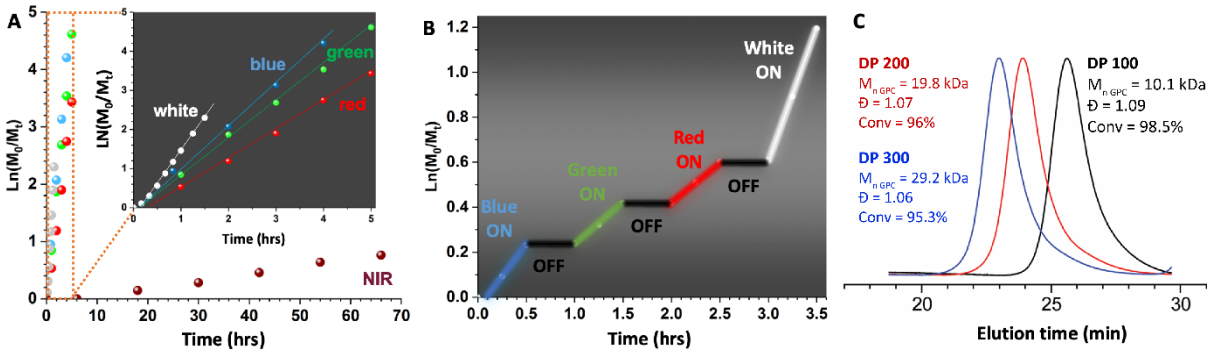

Author Manuscript

This article is protected by copyright. All rights reserved

3. authors claimed well controlled under air but the dispersity was 1.6. Is this really strong controlled?

Our manuscript mentions two polymerizations without degassing; the first is using SA-TCPP in water with blue light irradiation to polymerize DMA, which resulted in 67% conversion and a dispersity of 1.04 as shown in the supporting information Figure S6, which does show strong control.

The second instance is the polymerization of PEGMA in cell culture. Here we limit our claims to stating that polymerization was possible and do not claim strong control. The dispersity of 1.5 is likely due to the brush architecture and the monomer structure. PEGMA was used for the polymerization in cell culture because it is less toxic to cells than DMA. PEGMA itself is an oligomer with 8-9 ethylene glycol repeat units and is therefore already slightly dispersed. We have modified our description of GPC characterization as follows:

"The conversion of PEGMA was 11% and GPC characterization showed a monomodal peak with a small tail (Figure 4B)."

4. Perhaps end group analysis can complement information regarding the availability of the raft group in the living process. This also provides Mn which should be compared with GPC data. If there is a disagreement, then FRP terminates the chain growth.

The NMR spectrum of the final chain extension product with DP 300 has been added to the supporting information (Figure S9). Peak integration of the RAFT agent methyl groups and the polymer backbone show the polymer contains 289 DMA repeat units, giving Mn = 28.9 kDa, in close agreement with our GPC Mn of 29.2 kDa. These data along with the exquisite control shown throughout all DMA polymerizations including the chain extensions strongly demonstrate the continued availability of the RAFT group and that FRP is not terminating chain growth.

5. in the on/off cycles, the different light sources showed different slopes although this should proceed according to 1st order. Please explain. Could it be that this is an effect caused by the different absorption and therefore different absorbed amount on photons?

We agree with the reviewer and should have addressed the difference in polymerization rates. As seen in Figure 2A, the rate of polymerization is greatest with white light, followed by blue, green, and then red. This is due to both the absorbance of SA-TCPP and because the energy of photons decreases as the wavelength increases. To make sure this is clear to the reader, the following sentence has been added to the text:

"Pleasingly, the rates of polymerization during the "on" periods were in agreement with those observed in Figure 2A, with white light showing the greatest rate of polymerization, followed by blue, green, and red."

After answering the questions line by line the ms can be published.

The first author of ref. 14a will happy to see correct spelling of the last name. The second character is an ü (u as umlaut). Kütahya is correct spelling.

Thank you for noticing this error and we apologize for the oversight. The reference now contains the correct spelling.

Author Manuscript

This article is protected by copyright. All rights reserved

Reviewer 2:

Dynamic modulation of CRP by external stimuli has gained a great deal of attention as they grant the ability to control a polymerization spatially and temporally. However, NIR photocatalysts that can effect CRP under biologically benign conditions are lacking but are of high importance to push this technology forward. In this manuscript, Qiao and co-workers describe the first NIR-mediated CRP in aqueous conditions. The novel catalyst has broadband absorption, enabling CRP to be conducted under blue, green, red and NIR, covering the major portion of solar spectrum. In particular, the process is oxygen tolerant and can be conducted at microliter scale. The biocompatibility of this technology is further demonstrated in the presence of cells, though conditions need to be further optimized to improve cell viability.

I believe this is an importance advance in the field and the data reported is highly interesting. The manuscript is very well written and the conclusion is fully supported by data. I recommend this work be published as a VIP and suggest the authors consider the following for revision.

1. Provide absorption spectrum for molecularly dissolved TCPP, possibly in an organic solvent, for comparison with that of SA-TCPP. This helps validate the necessity for use of the microparticulate form to achieve broadband photocatalyst.

The following figure showing the absorbance of TCPP in DMF and SA-TCPP in water has been added to the SI to clearly show the broader absorbance of SA-TCPP photocatalyst. (Figure S1):

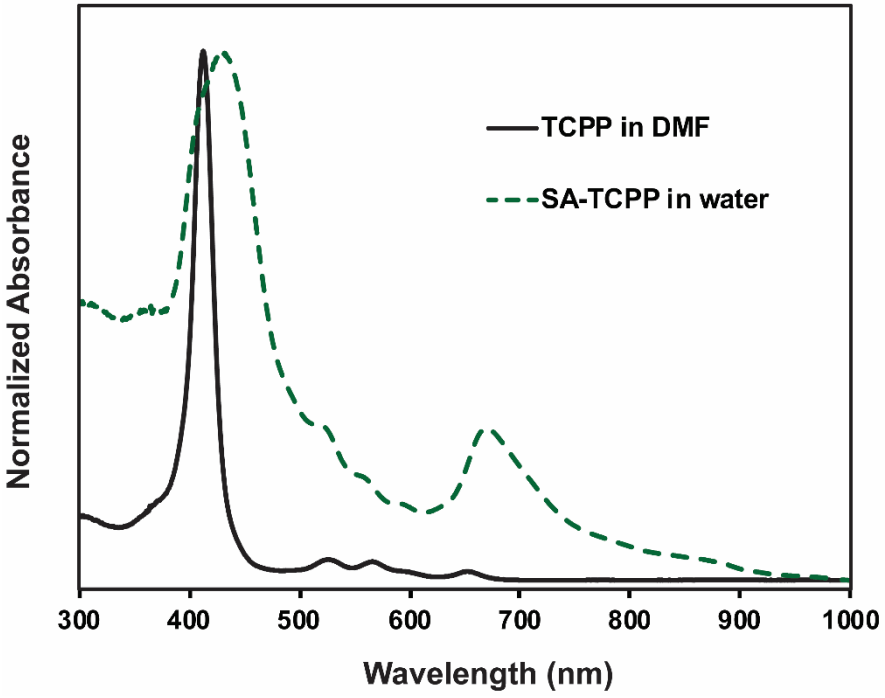

2. Provide a description of the size features of SA-TCPP and its state of existence in solution.

Because the SA-TCPP is a self-assembled structure that does not dissolve in water, the scanning electron microscopy (SEM) images provide a reasonable representation of the photocatalyst size features in water. A representative SEM image was further analysed using ImageJ. Analysis of the SA-TCPP fibres demonstrated

Author Manuscript

This article is protected by copyright. All rights reserved

the length of the self-assembled structures is highly variable (3.0 ± 2.09 μm), although the width is more consistent (0.13 ± 0.05 μm). This has been added to the supporting information as Figure S2.

3. For comparison of the performance of different photocatalysts, please specify the solvents (organic or water) and the amount of photocatalysts loaded. Since the authors said the other previously reported photocatalyst nanomaterials are hydrophobic but SA-TCPP was produced in water, the effect of solvents should be ruled out for photocatalyst comparison.

All reactions were performed in water, using 2.5 mg/mL photocatalyst unless otherwise stated. Any differences in polymerization are therefore due to the catalyst activity and not solvent effects. To clarify this for the reader, the solvent has been added to the Figure S7 figure title and the following sentence in the main text has been modified:

"The broad absorption spectrum of SA-TCPP allowed us to investigate its efficiency in comparison to previously reported H_2 evolution photocatalysts g-C_3N_4, CTF-1, and FAT, in water ([photocatalyst] = 2.5 mg mL^{-1}) under blue, green, and red light irradiation (Figure S7)."

4. Since SA-TCPP is prepared in water but polymerization is conducted in 50% DMA solution, I wonder if the nanostructure (morphology or size) is changed after polymerization.

This is an interesting question. During the set up and polymerization we did not observed any change in the appearance of the SA-TCPP photocatalyst, which is a different colour than the non-self-assembled TCPP. Kinetics also show the catalyst maintained its activity until full conversion was achieved. With these facts in mind, we do not believe any significant change to the photocatalyst occurred.

5. Scheme 1, TEOA with an oxidation potential of ~0.84 V vs SCE (Polym. Chem., 2019, 10, 2801-2811) is typically used as an electron donor. This is also expected to be the case in this study considering the energy gap of SA-TCPP. So a positive charge, not a negative charge, should be generated on TEOA.

Thank you for pointing out this error. Scheme 1 has been corrected to reflect the positive charge on TEOA.

6. Please provide molecular data for Figure 2C.

As mentioned in response to Reviewer 1 question 2, Figure 2C has been modified to include the $M_{n\ GPC}$, dispersity, and conversion of the chain extension polymers.

7. Biocompatible photopolymerization is interesting. Given high biocompatibility typically needs low concentrations of monomers and catalysts and oxygen tolerance is related to solution volume, such information needs to be clearly described in the text.

Thank you for your feedback. To address this issue, the following sentence has been added to the main text to describe the reagents:

"Six wells each contained 0.13 mg SA-TCPP, 22 mg PEGMA, 0.7 mg TTC, and 0.5 mg TEOA in complete DMEM cell culture medium to a total volume of 100 μL."

Author Manuscript

This article is protected by copyright. All rights reserved

8. Another interesting direction for oxygen tolerant photopolymerization is the recent exploration of photoenzymes for CRP. This represents an important conceptual advance and can be cited in the background introduction (see Angew. Chem. Int. Ed., 2019, 58(28), 9479-9484)

Thank you for bringing this exciting paper to our attention. The following sentence has been added to the introduction:

"Interestingly, a photoenzymatic RAFT mechanism using flavin-dependent enzymes was recently reported, with visible light causing photoexcitation of $FADH^-$ to facilitate the PET process and mediate polymerization.[8]"

We appreciate the feedback from the reviewers and their insights are reflected in this improved version of our manuscript. This manuscript presents significant progress in broadband- and NIR-mediated controlled radical polymerizations, an urgent finding which should appeal to the broad readership of *Angewandte Chemie* and is supported by the high importance rating from the reviewers. We have shown synthesis of precision polymers using a specially designed photocatalyst under blue, green, red, and NIR light irradiation. We also made initial exploitation of the oxygen tolerance and aqueous nature of our system to demonstrate such polymerization can be conducted in mammalian cell culture wells at the microliter scale, highlighting the opportunities for future biocompatible polymerization.

We can confirm that these results have not been published elsewhere. Thank you for considering this submission for publication and please let me know if you require any further information.

Kind Regards,

Greg Qiao

Author Manuscript

This article is protected by copyright. All rights reserved

From UV to NIR: A full spectrum metal-free photocatalyst for efficient polymer synthesis in aqueous conditions

Stephanie Allison-Logan,[a] Qiang Fu,*[,a,b] Yongkang Sun,[a] Min Liu,[a] Jijia Xie,[c] Junwang Tang,*[,c] and Greg G Qiao*[,a]

[a] S. Allison-Logan, Dr Q. Fu, Y. Sun, M. Liu, Prof G.G. Qiao
Polymer Science Group, Department of Chemical Engineering
University of Melbourne
Parkville, VIC 3010, Australia
E-mail: greggh@unimelb.edu.au

[b] Dr Q. Fu
Centre for Technology in Water and Wastewater (CTWW), School of Civil and Environmental Engineering
University of Technology Sydney
Ultimo, NSW 2007, Australia
E-mail: qiang.fu@uts.edu.au

[c] Dr J. Xie, Prof J. Tang
Solar Energy & Advanced Materials Research Group, Department of Chemical Engineering
University College London
Torrington Place, London WC1E JE, United Kingdom
E-mail: junwang.tang@ucl.ac.uk

Supporting information for this article is given via a link at the end of the document.

Abstract: Photo-mediation offers unparalleled spatiotemporal control over controlled radical polymerizations (CRP). Photo-induced electron/energy transfer reversible addition-fragmentation chain transfer (PET-RAFT) polymerization is particularly versatile due to its oxygen tolerance and wide range of compatible photocatalysts. In recent years, broadband- and near-infrared (NIR)-mediated polymerizations have been of particular interest due to their potential for solar-driven chemistry and biomedical applications. In this work, we present the first example of a novel photocatalyst for both full broadband- and NIR-mediated CRP in aqueous conditions. Well-defined polymers were synthesized in water under blue, green, red, and NIR light irradiation. Exploiting the oxygen tolerant and aqueous nature of our system, we also report PET-RAFT polymerization at the microliter scale in a mammalian cell culture medium.

Photo-mediation enables spatiotemporal control of controlled/living radical polymerizations (CRP) while maintaining excellent dispersity and chain-end fidelity.[1] For this reason, visible light-mediated reversible addition-fragmentation chain transfer (RAFT) polymerization has been studied extensively since its discovery in 2014.[2] Such RAFT polymerization encompasses two distinct mechanisms known as photoiniferter and photo-induced electron/energy transfer (PET)-RAFT approaches. Photoiniferter RAFT polymerization requires direct activation of the RAFT agent via light irradiation and is therefore limited to wavelengths absorbed by the RAFT agent, generally UV, blue, or green light.[3] The PET-RAFT mechanism depends on the excitation of a photoredox catalyst or a photosensitiser by light irradiation. The excited catalyst/photosensitizer interacts with the RAFT agent via energy or electron transfer to generate the initiating radical for polymerization.[2, 4] Numerous compounds have been employed as photoredox catalysts or photosensitizers for PET-RAFT polymerization including organic dyes,[5] metalloporphyrins such as zinc tetraphenylporphyrin (ZnTPP),[6] naturally-occurring photosynthetic pigments,[7] enabling PET-RAFT polymerization across the visible light spectrum. Interestingly, a photoenzymatic RAFT mechanism using flavin-dependent enzymes was recently reported, with visible light causing photoexcitation of $FADH^-$ to facilitate the PET process and mediate polymerization.[8] In addition, PET-RAFT polymerization is typically less sensitive to oxygen and can therefore be performed under less stringent conditions.[8-9]

As PET-RAFT polymerization has gained popularity due to its versatility and less stringent reaction conditions, there has been a push to develop photocatalysts with broadband and near-infrared (NIR) absorption, due to potential "green" chemistry and biomedical applications. The solar spectrum covers wavelengths from 250-2500 nm, with IR energy alone making up nearly 50% of solar energy, while photons from visible light and NIR constitute 95% of the solar flux at sea level.[10] Therefore, broadband and NIR absorbance are necessary to achieve efficient solar energy utilisation. In addition, NIR can penetrate opaque materials including human tissues, and therefore has potential use in biomedical applications and even *in vivo* polymerization.[11] Boyer and coworkers reported the first NIR-mediated CRP, using bacteriochlorophyll a as a photocatalyst.[12] More recently, they reported the use of aluminum napthalocyanine as a photosensitizer for peroxides to initiate RAFT polymerization under NIR irradiation.[13] The authors demonstrated temporal control and achieved high conversions even with paper, chicken skin, and pig skin barriers. These reports are significant developments in NIR-mediated photopolymerization and potential *in vivo* polymerization but to date have been limited to organic solvent.

Focusing on broadband photopolymerization, Matyjaszewski and coworkers exploited the localized surface plasmon resonance (LSPR) effect of nanostructured silver orthophosphate (Ag_3PO_4) photocatalysts.[14] PET-RAFT polymerization of methyl acrylate demonstrated high conversions following blue, green, and red light irradiation in as well as when exposed to natural sunlight. In addition, polymerization of benzyl acrylate was possible using NIR irradiation. However, polymerization was again only limited to organic solvent.

Author Manuscript

This article is protected by copyright. All rights reserved

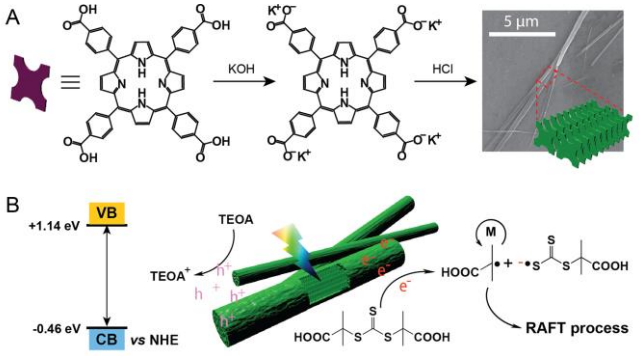

Scheme 1. (A) The synthetic strategy for rod-like SA-TCPP and (B) schematic mechanism of the photocatalytic PET-RAFT polymerizations by SA-TCPP.

To date, all NIR-mediated CRP polymerization systems reported have been employed in organic solvents.[12-15] However, the development of aqueous systems is essential for any potential *in vivo* applications and could also offer less expensive and more environmentally friendly options for industrial use. To aid with the development of aqueous broadband- and NIR-responsive systems, we looked to recent advances in the field of photocatalysis for solar-driven hydrogen evolution. Our group has previously reported efficient PET-RAFT polymerization with organic semiconductor graphitic carbon nitride (g-C_3N_4),[16] an organic photocatalyst previously used in hydrogen evolution.[17] With the use of g-C_3N_4, RAFT polymerization can be carried out with no degassing or monomer purification.[16] Due to the limited absorbance spectrum and relatively hydrophobic surface functional groups of g-C_3N_4, its activity for polymerizations was only studied under UV irradiation in DMSO. More recently, novel photocatalysts such as covalent triazine-based framework-1 (CTF-1)[18] and formic acid-treated carbon nitride (FAT)[19] have shown narrower band gaps and red-shifted absorbance spectra in comparison to g-C_3N_4. Due to the improved function of these new catalysts, our previous successful PET-RAFT polymerizations using g-C_3N_4, and the need of aqueous PET-RAFT systems under NIR, we decided to investigate the use of these photocatalysts for PET-RAFT polymerization under various wavelengths in an aqueous system.

In addition, we synthesized a novel self-assembled carboxylated porphyrin (SA-TCPP) photocatalyst. Although it has been previously shown that nanometric SA-TCPP particles had a high solar spectrum efficiency and enhanced hydrogen and oxygen evolution from water under visible light irradiation,[20] our prepared micro-size SA-TCPP photocatalyst displayed a broader absorbance spectrum from 300 to 950 nm (Figure 1A and S1). Due to the micro-fibre like morphology, the lifetime of photoexcited electron-hole pairs is further extended, which in turn can lead to an improved polymerization efficiency compared to other recently reported photocatalysts for hydrogen evolution. As our PET-RAFT polymerization with this catalyst is in aqueous conditions under broad wavelengths, we further tested its polymerization ability in biological cell culture media, investigating its potential for *in situ* biomedical applications as well as highly efficient "green" controlled polymerizations.

We prepared the SA-TCPP photocatalyst through a modified approach. Commercially available 5,10,15,20-tetra (4-carboxyphenol) porphyrin (TCPP) was deprotonated in an aqueous 1M KOH solution and heated to 80 °C, yielding a purple solution. 0.1M HCl was added dropwise until the pH became neutral, following which the precipitate was purified via dialysis and freeze-dried. The resultant self-assembled TCPP (SA-TCPP) showed a dark green colour and formed long fibres/rods as seen using SEM (Scheme 1 and Figure S2). The obtained rods displayed a non-crystalline X-ray diffraction (XRD) pattern and this result was further confirmed by TEM diffraction measurement (Figure 1B). Two obvious peaks at 7° and 22° represent the 1.26 nm width of an aggregated TCPP molecule and the 0.4 nm face-to-face distance between TCPP molecules. X-ray photoelectron spectroscopy (XPS) peaks assigned to carbon 1s, nitrogen 1s, and oxygen 1s were located at 285, 400, and 533 eV, respectively, and were consistent with the molecular structure of SA-TCPP (Figures 1C and S4). Furthermore, the electrochemical experiment further revealed that the prepared SA-TCPP rods exhibit a band gap of -0.46 to +1.14 eV (Figure S5).

The broad absorption spectrum of SA-TCPP allowed us to investigate its efficiency in comparison to previously reported H_2 evolution photocatalysts g-C_3N_4, CTF-1, and FAT, in water ([photocatalyst] = 2.5 mg mL^{-1}) under blue, green, and red light irradiation (Figure S7). In all cases, polymerizations performed with SA-TCPP resulted in the highest conversion. All polymerizations showed linear semi-logarithmic plots and dispersities of 1.1 or below. While all polymerizations achieved high conversions under blue light irradiation, SA-TCPP increasingly outperformed the other catalysts as the irradiation wavelength increased and was the only catalyst that led to polymer formation under red light irradiation (Figure 1D).

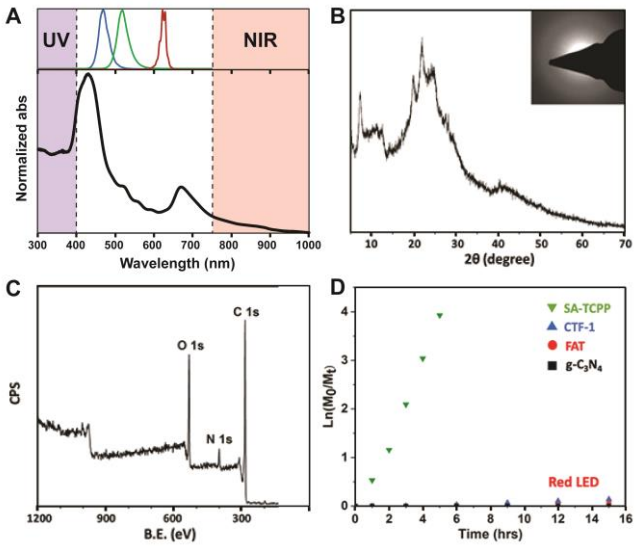

Figure 1. (A) UV-vis normalized absorption spectrum of SA-TCPP (bottom) and LED light source emission spectra (top). (B) XRD and electron diffraction patterns of SA-TCPP. (C) Full XPS spectrum of SA-TCPP. (D) Polymerization kinetics of DMA using SA-TCPP and previously reported photocatalysts under red light irradiation.

The polymerization kinetics of DMA using SA-TCPP under blue, green, red, white, and NIR irradiation are shown in Figure 2A. The use of CTF-1, FAT, and g-C_3N_4 was not investigated under NIR irradiation due to their limited absorbance spectra and poor performance under red light. In a typical reaction,

Author Manuscript

This article is protected by copyright. All rights reserved

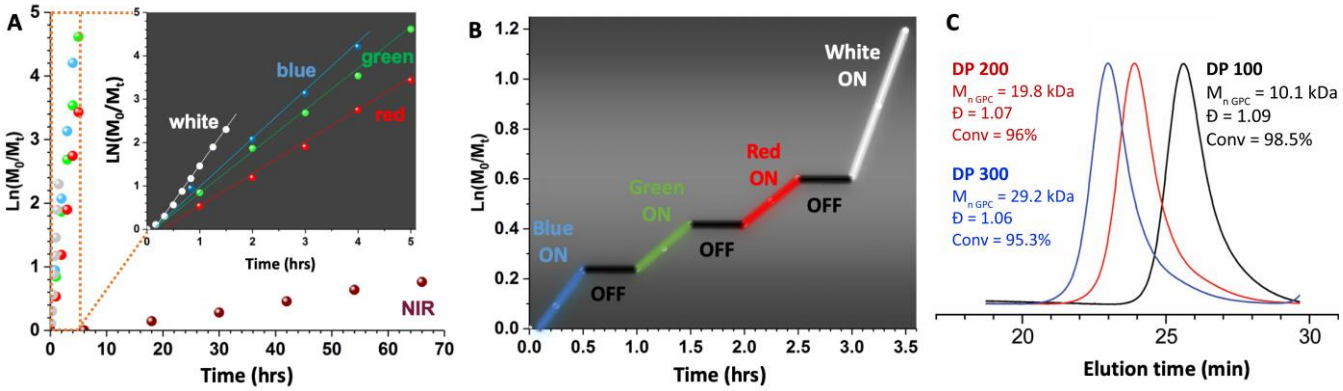

Figure 2. Kinetics of SA-TCPP-catalyzed RAFT polymerizations of DMA under (A) various LED irradiation (white to NIR, 4 mW/cm^2) and (B) in an "ON/OFF" experiment. (C) GPC evolution of a *pseudo*-pentablock PDMA by chain extension.

DMA (100 equivalents), trithiocarbonate (TTC) RAFT agent (1 equivalent), triethanolamine (TEOA, 13.4 equivalents) and SA-TCPP (5 mg) were dissolved in DI water (50 % v/v). Reaction mixtures were bubbled with argon for 20 minutes prior to light irradiation to afford faster polymerization and reduced induction period, although degassing and addition of TEOA were not essential, as previously reported (Figure S8).[16]

The rate of polymerization was highest using white light, followed by blue, green, red, and NIR (Figure 2A). Monomer conversions of 90% or greater were achieved in 90 min using white light, 3 h with blue or green light, and 4 h with red light. Although the NIR-mediated polymerization was significantly slower, 53% conversion was reached in 66 h. These results are consistent with the absorbance spectrum of SA-TCPP shown in Figure 1A, where absorbance was greatest at blue-shifted wavelengths, as well as the higher energy of lower wavelength photons. In all cases, linear pseudo-logarithmic plots were observed indicating a constant radical concentration.

The temporal control of the system was then demonstrated using an "on/off" experiment, where the light source was turned on and off at 30 minute intervals (Figure 2B). Several cycles were performed with a different wavelength of light used during each "on" period, highlighting the broadband absorption of the photocatalyst. No polymerization was observed during the off period, demonstrating instantaneous temporal control. After 2 hours of irradiation, 70% monomer conversion was achieved. Pleasingly, the rates of polymerization during the "on" periods were in agreement with those observed in Figure 2A, with white light showing the fastest rate of polymerization, followed by blue, green, and red.

Crucially, retention of the TTC RAFT agent and its living nature were demonstrated via two chain extension reactions with greater than 95% monomer conversion attained for each block (Figures 2C and S9). GPC traces showed symmetrical, monomodal peaks after each chain extension. Due to the symmetrical nature of the RAFT agent employed (S,S'-Bis(α, α'-dimethyl- α"-acetic acid)trithiocarbonate), the TTC moiety remained at the centre of the polymer and the two chain extensions experiments resulted in a well-defined *pseudo*-pentablock polymer.

Successful NIR-mediated polymerization with SA-TCPP suggested PET-RAFT polymerization could be performed through barriers. NIR is known to penetrate barriers, including mammalian tissues, and the Boyer and Matyjaszewski groups have previously reported successful NIR-mediated PET-RAFT polymerization through materials such as paper and animal skin.[13-14] Interestingly, Boyer and coworkers observed minimal change in the apparent rate propagation coefficient when polymerizing methyl acrylate through 0.1 mm paper, 1 mm chicken skin, and 2.5 mm pig skin barriers, mediated by NIR (850 nm).[13]

Therefore, we set out to determine if we could perform our polymerization through a barrier using NIR (850 nm) and SA-TCPP in an aqueous environment. We carried out our investigation using a piece of opaque paper wrapped around the reaction vessel as a barrier. An induction period of 6 hours was observed before achieving 30% conversion after 66 h (Figure 3B). The GPC trace of the resulting polymer was monomodal and symmetrical, with a low dispersity of 1.07, as shown in Figure 3C. To our knowledge, this is the first time NIR irradiation has been used for CRP polymerization in water. These results signify an essential step towards biocompatible NIR-mediated polymerization, where an aqueous system would be essential.

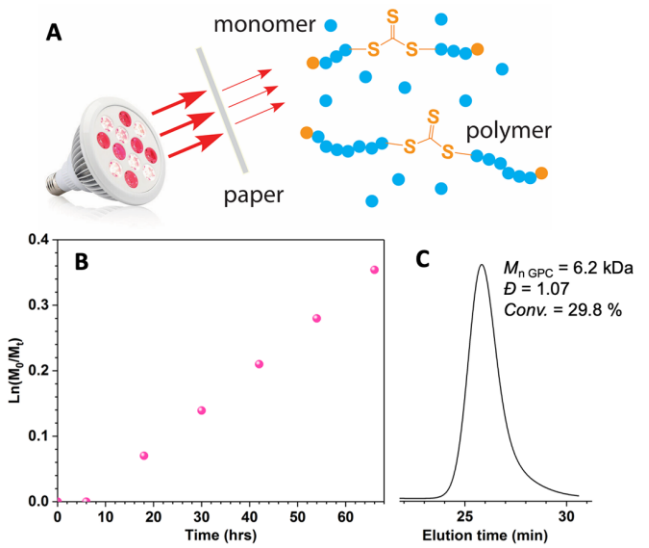

Figure 3. (A) Schematic illustration of an opaque paper barrier employed for polymerizations under NIR LED light (λ_{max} = 850 nm). (B) Kinetic study of SA-TCPP catalyzed RAFT polymerization of DMA under NIR LED irradiation (4 mW/cm^2). (C) GPC curve of the resultant PDMA.

Author Manuscript

This article is protected by copyright. All rights reserved

Any in vivo polymerizations would also need to be biocompatible and performed with a low volume. To this end, we attempted a preliminary study of the PET-RAFT polymerization using PEG methacrylate (PEGMA, 480 Da) in the presence of mammalian fibroblast cells in a 96-well plate (Figure 4A). Six wells each contained 0.13 mg SA-TCPP, 22 mg PEGMA, 0.7 mg TTC, and 0.5 mg TEOA in complete DMEM cell culture medium to a total volume of 100 µL. The 96-well plate was irradiated with red light for 45 minutes at 37 °C. The conversion of PEGMA was 11% and GPC characterization showed a monomodal peak with a small tail (Figure 4B). Significantly, this work demonstrates our system can conduct polymerization without degassing at microlitre scale, offering the future potential for machine programable multi-block polymerization via computer-controlled microliter injection systems. We also measured cell viability immediately following light irradiation and obtained 46% cell viability (Figure 4C). While optimization of reaction conditions and reagents is needed to reduce the toxicity of the system, these preliminary results suggest a biocompatible, NIR-mediated PET-RAFT polymerization may soon be possible.

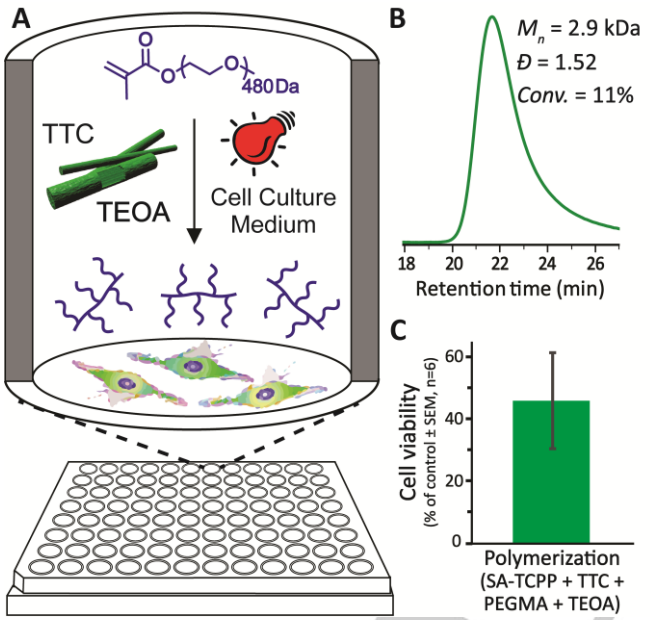

Figure 4. (A) Microliter-scale PET-RAFT polymerization of $PEGMA_{480}$ in a 96-well plate containing fibroblast cells, 45 minutes red light irradiation. (B) GPC trace of poly (PEGMA), and (C) cell viability following PET-RAFT polymerization.

The recent reports by the Boyer,[12-13] Matyjaszewski,[14] and Yagci[15a] groups demonstrate exciting developments in broadband- and NIR-mediated CRP. Building on these critical advances, we report for the first time an aqueous NIR-mediated CRP. The use of a metal-free, porphyrin-based organic photocatalyst with an absorbance spectrum covering 300-950 nm enabled broadband- and NIR-mediated PET-RAFT polymerization in water. SA-TCPP was compared to three other photocatalysts previously reported for hydrogen evolution and was found to have the highest rate of polymerization when irradiated with white, blue, green, and red light. Preliminary investigations resulted in the successful microliter-scale polymerization of PEGMA in the presence of mammalian cells in complete cell culture medium, with future works to focus on improving cell viability. These findings have broad implications for potential *in vivo* polymerizations for biomedical applications as well as "green" polymerizations.

Acknowledgements

G.G.Q. acknowledges the Australian Research Council's Discover Project (DP170104321). S.A.-L. is the recipient of a Melbourne International Engagement Award. M.L. acknowledges support from the China Scholarship Council-University of Melbourne Research Scholarship (201606260063). Q.F. acknowledges the Australian Research Council under the Future Fellowship (FT180100312). J.X. and J.T. are thankful for the financial support from the Royal Society Newton Advanced Fellowship grant (NAF\R1\191163) and Leverhulme Trust (RPG-2017-122).

Keywords: RAFT polymerization • photocatalysis • NIR • photopolymerization

[1] a) T. G. McKenzie, Q. Fu, M. Uchiyama, K. Satoh, J. Xu, C. Boyer, M. Kamigaito, G. G. Qiao, *Adv. Sci.* **2016**, *3*, 1500394; b) N. D. Dolinski, Z. A. Page, E. H. Discekici, D. Meis, I. H. Lee, G. R. Jones, R. Whitfield, X. Pan, B. G. McCarthy, S. Shanmugam, *J. Polym. Sci., Part A: Polym. Chem.* **2019**, *57*, 268-273.

[2] J. Xu, K. Jung, A. Atme, S. Shanmugam, C. Boyer, *Journal of the American Chemical Society* **2014**, *136*, 5508-5519.

[3] a) T. G. McKenzie, Q. Fu, E. H. Wong, D. E. Dunstan, G. G. Qiao, *Macromolecules* **2015**, *48*, 3864-3872; b) J. Yeow, O. R. Sugita, C. Boyer, *ACS Macro Lett.* **2016**, *5*, 558-564; c) S. b. Perrier, *Macromolecules* **2017**, *50*, 7433-7447.

[4] N. Corrigan, J. Xu, C. Boyer, X. Allonas, *ChemPhotoChem* **2019**, *3*, 1193-1199.

[5] a) C. A. Figg, J. D. Hickman, G. M. Scheutz, S. Shanmugam, R. N. Carmean, B. S. Tucker, C. Boyer, B. S. Sumerlin, *Macromolecules* **2018**, *51*, 1370-1376; b) S. Shanmugam, S. Xu, N. N. M. Adnan, C. Boyer, *Macromolecules* **2018**, *51*, 779-790; cJ. Xu, S. Shanmugam, H. T. Duong, C. Boyer, *Polym. Chem.* **2015**, *6*, 5615-5624; dN. Corrigan, L. Zhernakov, M. H. Hashim, J. Xu, C. Boyer, *React. Chem. Eng.* **2019**, *4*, 1216-1228.

[6] a) A. J. Gormley, J. Yeow, G. Ng, Ó. Conway, C. Boyer, R. Chapman, *Angew. Chem. Int. Ed.* **2018**, *57*, 1557-1562; b)K. Satoh, Z. Sun, M. Uchiyama, M. Kamigaito, J. Xu, C. Boyer, *Polym. J.* **2019**, 1-9; c) M. Li, M. Fromel, D. Ranaweera, S. Rocha, C. Boyer, C. Pester, *ACS Macro Lett.* **2019**, *8*, 374-380; d) P. Seal, J. Xu, S. De Luca, C. Boyer, S. C. Smith, *Adv. Theory Simul.* **2019**, *2*, 1900038.

[7] a) S. Shanmugam, J. Xu, C. Boyer, *Chemical Science* **2015**, *6*, 1341-1349; b) J. M. Ren, T. G. McKenzie, Q. Fu, E. H. Wong, J. Xu, Z. An, S. Shanmugam, T. P. Davis, C. Boyer, G. G. Qiao, *Chemical Reviews* **2016**, *116*, 6743-6836; c) C. Wu, S. Shanmugam, J. Xu, J. Zhu, C. Boyer, *Chem. Commun.* **2017**, *53*, 12560-12563.

[8] F. Zhou, R. Li, X. Wang, S. Du, Z. An, *Angewandte Chemie International Edition* **2019**, *58*, 9479-9484.

[9] a) L. Zhang, C. Wu, K. Jung, Y. H. Ng, C. Boyer, *Angew. Chem. Int. Ed.* **2019**, *131*, 16967-16970; b) N. Zaquen, A. M. Kadir, A. Iasa, N. Corrigan, T. Junkers, P. B. Zetterlund, C. Boyer, *Macromolecules* **2019**, *52*, 1609-1619.

[10] a) M. Q. Yang, M. Gao, M. Hong, G. W. Ho, *Adv. Mater.* **2018**, *30*, 1802894; b) L. Liang, X. Li, Y. Sun, Y. Tan, X. Jiao, H. Ju, Z. Qi, J. Zhu, Y. Xie, *Joule* **2018**, *2*, 1004-1016.

[11] N. Corrigan, J. Yeow, P. Judzewitsch, J. Xu, C. Boyer, *Angew. Chem. Int. Ed.* **2019**, *58*, 5170-5189.

Author Manuscript

This article is protected by copyright. All rights reserved

[12] S. Shanmugam, J. Xu, C. Boyer, *Angew. Chem. Int. Ed.* **2016**, *55*, 1036-1040.
[13] Z. Wu, K. Jung, C. Boyer, *Angew. Chem. Int. Ed.* **2020**, *59*, 2013-2017.
[14] J. Jiang, G. Ye, F. Lorandi, Z. Liu, Y. Liu, T. Hu, J. Chen, Y. Lu, K. Matyjaszewski, *Angew. Chem. Int. Ed.* **2019**, *58*, 12096-12101.
[15] a) C. Kütahya, C. Schmitz, V. Strehmel, Y. Yagci, B. Strehmel, *Angew. Chem. Int. Ed.* **2018**, *57*, 7898-7902; b)C. Tian, P. Wang, Y. Ni, L. Zhang, Z. Cheng, X. Zhu, *Angew. Chem. Int. Ed. Engl.* **2020**, *59*, 3910-3916.
[16] Q. Fu, Q. Ruan, T. G. McKenzie, A. Reyhani, J. Tang, G. G. Qiao, *Macromolecules* **2017**, *50*, 7509-7516.
[17] X. Wang, K. Maeda, A. Thomas, K. Takanabe, G. Xin, J. M. Carlsson, K. Domen, M. Antonietti, *Nat. Mater.* **2009**, *8*, 76-80.
[18] J. Xie, S. A. Shevlin, Q. Ruan, S. J. A. Moniz, Y. Liu, X. Liu, Y. Li, C. C. Lau, Z. X. Guo, J. Tang, *Energy Environ. Sci.* **2018**, *11*, 1617-1624.
[19] Y. Wang, F. Silveri, M. K. Bayazit, Q. Ruan, Y. Li, J. Xie, C. R. A. Catlow, J. Tang, *Adv. Energy Mater.* **2018**, *8*, 1801084.
[20] Z. Zhang, Y. Zhu, X. Chen, H. Zhang, J. Wang, *Adv. Mater.* **2019**, *31*, e1806626.

WILEY-VCH

Author Manuscript

This article is protected by copyright. All rights reserved

Entry for the Table of Contents

Insert graphic for Table of Contents here.

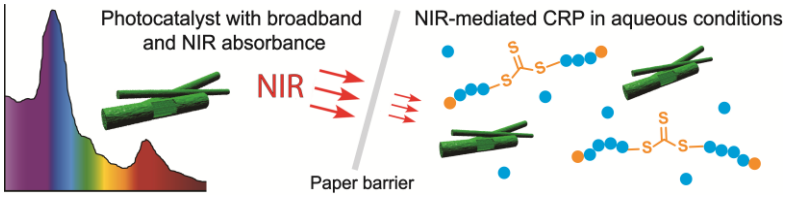

Insert text for Table of Contents here.

Photopolymerizations mediated by broadband and near-infrared (NIR) light are of intense interest due to their potential use in solar-driven and *in vivo* applications. Employing a novel metal-free photocatalyst and PET-RAFT approach, we present the first broadband- and NIR-mediated controlled radical polymerization in aqueous media, including cell culture medium, marking a crucial advance towards *in vivo* polymerization for biomedical applications.

Author Manuscript

This article is protected by copyright. All rights reserved

From UV to NIR: A full spectrum metal-free photocatalyst for efficient polymer synthesis in aqueous conditions

Stephanie Allison-Logan,[a] Qiang Fu,*[,a,b] Yongkang Sun,[a] Min Liu,[a] Jijia Xie,[c] Junwang Tang,*[,c] and Greg G Qiao*[,a]

[a] Polymer Science Group, Department of Chemical Engineering, University of Melbourne, Parkville, VIC 3010, Australia

[b] Centre for Technology in Water and Wastewater (CTWW), School of Civil and Environmental Engineering, University of Technology Sydney, Ultimo, NSW 2007, Australia

[c] Solar Energy & Advanced Materials Research Group, Department of Chemical Engineering, University College London, Torrington Place, London WC1E JE, United Kingdom

Author Manuscript

Supporting Information

Materials

Tetra(4-carboxyphenyl)porphyrin (TCPP), *N*,*N*-dimethylacrylamide (DMA, 99%) and triethanolamine (TEOA, 98%) were purchased from Sigma-Aldrich and used as received. Hydrochloric acid, potassium hydroxide and dimethyl sulfoxide (DMSO) were purchased from Chem-Supply Pty Ltd and used as received. Snakeskin dialysis tubing (3.5k, MWCO) was purchased from Thermo Fisher Scientific. The White-Red-Green-Blue RGB waterproof LED strip lighting 5050 was used for PET-RAFT experiments (DC12V, 4.0 mW cm^{-2}). The LED light emission spectra (blue: λ_{max} ~ 465 nm, green: λ_{max} ~ 520 nm, and red: 630 nm, respectively) were measured using a Maya 2000Pro spectrometer fitted with optical fiber 139 (OceanOptics 100UV). Chain transfer agent S,S'-bis(α, α'-dimethyl-α"-acetic acid)trithiocarbonate (CTA) was synthesized as previously reported.[1] Photocatalysts graphitic carbon nitride (g-C_3N_4), covalent triazine-based framework-1 (CTF-1), and formic acid-treated carbon nitride (FAT) were synthesized as previously reported.[2-5] Dulbecco's Modified Eagle Medium (DMEM), fetal bovine serum (FBS), GlutaMAX, penicillin, streptomycin, and trypsin-EDTA (1×) were purchased from Gibco, Invitrogen. Cell Counting Kit-8 was purchased from Sigma-Aldrich and used as instructed.

Characterization

Scanning Electron Microscopy (SEM). SEM measurements conducted on a Quanta FEG 200 ESEM. Samples were coated with gold using a Dynavac Mini Sputter Coater prior to imaging.

Transmission Electron Microscopy (TEM). TEM measurements were performed on a FEI Tecnai F20 microscope equipped with an EDAX TEAMTM EDS System.

Powder X-Rray Diffraction (PXRD). XRD pattern of the samples was recorded on a Bruker D8 Advance instrument with Cu Ka radiation (40 kV, 40 mA) and a nickel filter, and the samples were exposed at a scanning rate of $2\theta = 0.020$ s^{-1} in the range of 5-70°.

X-ray Photoelectron Spectroscopy (XPS). XPS was carried out on a VG ESCALAB 220i-XL spectrometer under ultra-high vacuum conditions (6×10^{-9} mbar) with fixed photon energy (A1 Kα 1486.6 eV). A survey scan was performed between 0 and 1200 eV with a resolution of 1.0 eV and pass energy of 100 eV. High resolution scans for C 1s (281 to 293 eV), O 1s (528 to 536

This article is protected by copyright. All rights reserved

eV) N 1s (396 to 405 eV) and Fe 2p (705 to 733 eV) were also conducted with a resolution of 0.05 eV and a pass energy of 20 eV.

Nuclear Magnetic Resonance (NMR) Spectroscopy. ^{1}H NMR spectroscopy was conducted on a Varian Unity 400 MHz spectrometer operating at 400 MHz, using the deuterated solvent ($CDCl_3$) as the reference and a sample concentration of approximately 10 mg·mL^{-1}.

Gel-Permeation Chromatography (GPC). The aqueous GPC system consisted of three Waters Ultrahydrogel columns in series ((i) 250 Å porosity, 6 µm bead size; (ii) and (iii) linear, 10 µm bead size). A Shimadzu RID-10 refractometer and Wyatt 3-angle MiniDawn light scattering detector were connected in series. Milli-Q water with 0.1 vol% TFA was used as eluent at a flow rate of 1 mL min^{-1} and the system operated at ambient temperature. For all PDMA polymers, dn/dc values were determined via a method of 100% mass recovery. Molecular weight and dispersity values were calculated using the Wyatt ASTRA software package from MALS data using a Debye model. Poly(PEGMA) dispersity values were calculated from PEG standards.

Absorbance of photocatalysts. The UV-Vis absorbance of SA-TCPP was recorded by measuring a dilute suspension of SA-TCPP in deionized water using a Shimadzu UV-2101 PC spectrophotometer. The absorption spectra of g-C_3N_4, CTF-1, and FAT were obtained in the solid state using a Shimadzu UV-Vis 2550 spectrophotometer fitted with an integrating sphere. Diffuse reflectance spectra were obtained using powdered samples, with standard barium sulphate powder as a reference. The reflection measurements were converted to absorption spectra via the Kubelka-Mulk transformation.

Methods

1. Synthesis of self-assembled Tetra(4-carboxyphenyl)porphyrin (SA-TCPP)

TCPP (500 mg) was dissolved in 20 mL of 1mol·L^{-1} KOH aqueous solution in a 500 mL round bottom flask. The mixture was then heated to 80 ^{o}C to afford a purple solution. Thereafter, 200 mL of 0.1 mol·L^{-1} HCl solution was added dropwise until the pH became neutral and no further precipitation was obtained. The prepared SA-TCPP was purified by dialysis against DI water using a regenerated cellulose dialysis tubing with a molecular weight cut-off of 3.5 kDa, followed by freeze-drying, yielding green powder.

2. Electrochemical measurements

A standard three-electrode cell was employed, with a working electrode (SA-TCPP), a saturated calomel electrode (SCE) as the reference electrode and a platinum wire as the counter electrode. Na_2SO_4 was taken as the electrolyte solution. All the potentials were given with reference to the SCE.

The working electrodes were prepared as follows: 5 mg SA-TCPP was suspended in 1 mL DI water under ultrasonication. A dark green slurry was obtained and drop-coated onto an indium tin oxide (ITO) glass electrode. Electrodes were dried in a vacuum oven at 60 ^{o}C.

3. General procedure for photoinduced electron transfer RAFT polymerization

A vial glass (7 mL) charged with photocatalysts (5 mg), DMA (1.03 mL, 10 mmol), CTA (28.2 mg, 0.1 mmol), TEOA (100 mg, 0.67 mmol), and DI water (50 vol %) ([DMA]/[CTA] = 100/1) was sealed with a rubber septa. The reaction mixture was degassed by bubbling Ar for 20 minutes. The LED light source (blue, green, red, or NIR; 4.0 mW cm^{-2}) was then switched "on", and the reaction mixture was stirred. Samples were taken at timed intervals *via* degassed syringe and immediately diluted with either DMSO-d_6 or DI water, for NMR and GPC analysis, respectively.

Author Manuscript

This article is protected by copyright. All rights reserved

4. "On/Off" reaction

The "on/off" reactions were set up in the same fashion; however, at a given reaction time the LED light source was turned off and the vial covered completely in aluminium foil and placed into a homemade "dark box" for 30 minutes. The polymerization was reactivated by irradiating the reaction mixture with LED light again. Samples were taken at timed intervals via degassed syringe and immediately diluted with either DMSO-d_6 or DI water for NMR and GPC analysis, respectively.

5. In situ chain extension

A 7 mL vial glass charged with SA-TCPP (5 mg), DMA (0.515 mL, 5 mmol), CTA (14.1 mg, 0.05 mmol), TEOA (100 mg, 6.7 mmol), and DI water (50 vol %) ([DMA]/[CTA] = 100/1) was sealed with a rubber septa. The vial was sparged with Ar for 20 min. The LED light source (white, 4.0 mW cm^{-2}) was then switched "on", and the reaction mixture was stirred. After 2 h the conversion of DMA achieves >95% by ^{1}H NMR analysis. The second portion of DMA monomer (0.515 mL, 5 mmol) and DI water was sparged with Ar for 20 min. The deoxygenated mixture was then injected into the reactor. After 2 hours, the monomer conversion achieved over 95% by ^{1}H NMR analysis. Finally, the last portion of the deoxygenated mixture containing 5 mmol DMA and DI water was injected into the reactor. After 4 hours, the monomer conversion achieved over 95% by ^{1}H NMR analysis. The sample was also taken and diluted with DI water for GPC analysis.

5. Cell Culture

NIH 3T3 mouse fibroblast cells were maintained in DMEM supplemented with 10% FBS, GlutaMAX (2mM), streptomycin (100 μg/mL) and penicillin (100 units/mL). Cells were passaged every 3-4 days using 0.25% trypsin-EDTA at subconfluence and incubated in a humidified incubator (37 °C, 5% CO_2, and 90% humidity). Cell passages 10-11 were used for experiments.

6. PET-RAFT polymerization in the presence of cells

NIH 3T3 cells seeded in a transparent, poly(styrene), flat-bottom 96-well plate (Corning) at 5×10^3 cells per well in supplemented DMEM cell culture medium. After 20 h the cell culture medium was replaced with 100 μL fresh medium (control wells) or medium containing PEGMA, TTC, TEOA, and/or SA-TCPP and irradiated with red light for 45 min at 37 °C, 5% CO_2, 90% humidity. Each treatment was performed in three or six separate wells as shown below:

Treatment/control (final concentration, in culture medium)	Number of wells
Blank (culture medium, no cells)	6
Control (culture medium)	6
SA-TCCP in culture medium (1.25 mg/mL)	3
PEGMA (20 μL), TEOA (50 mg/mL), TTC (7 mg/mL) in culture medium	3
SA-TCPP (1.25 mg/mL), PEGMA (20 μL), TEOA (50 mg/mL), and TTC (7 mg/mL), in culture medium	6

7. Cell viability assay

Cell viability was assessed using a standard Cell Counting Kit-8 (CCK-8) reagent. Following PET-RAFT polymerization, the treatment or cell culture medium was removed and each well was washed twice with 100 μL cell culture medium, followed by the addition of 100 μL cell culture medium and 10

Author Manuscript

This article is protected by copyright. All rights reserved

μL CCK-8 reagent. After 2 h incubation, the absorbance was measured using a Tecan M200 Infinite Pro microplate reader at a wavelength of 460 nm, reference wavelength 650 nm. Error bars represent the standard error of the mean, n=3 or n=6 as described above. The cell viability was calculated as a percent of the control using the following formula, where [A] is the absorbance:

$$Cell\ viability\ (\%\ of\ control) = \frac{[A]_{460\ (sample)} - [A]_{460\ (blank)}}{[A]_{460\ (control)} - [A]_{460\ (blank)}} \times 100\%$$

Additional Information

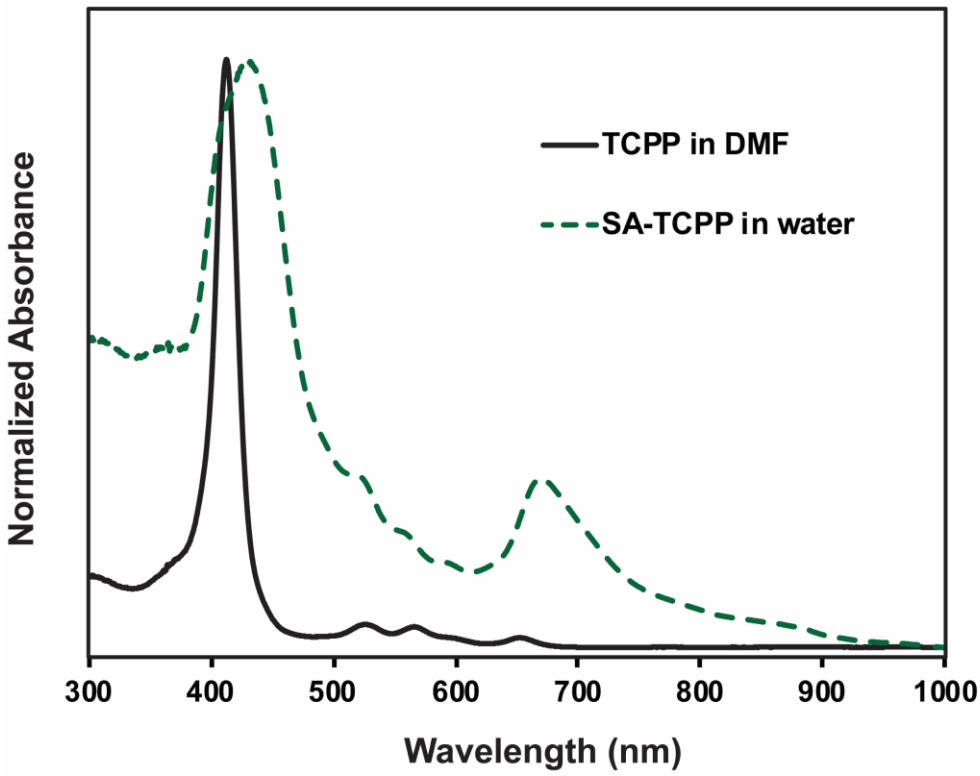

Figure S1. Normalized absorbance spectra of TCPP in DMF and the SA-TCPP photocatalyst in water.

Author Manuscript

This article is protected by copyright. All rights reserved

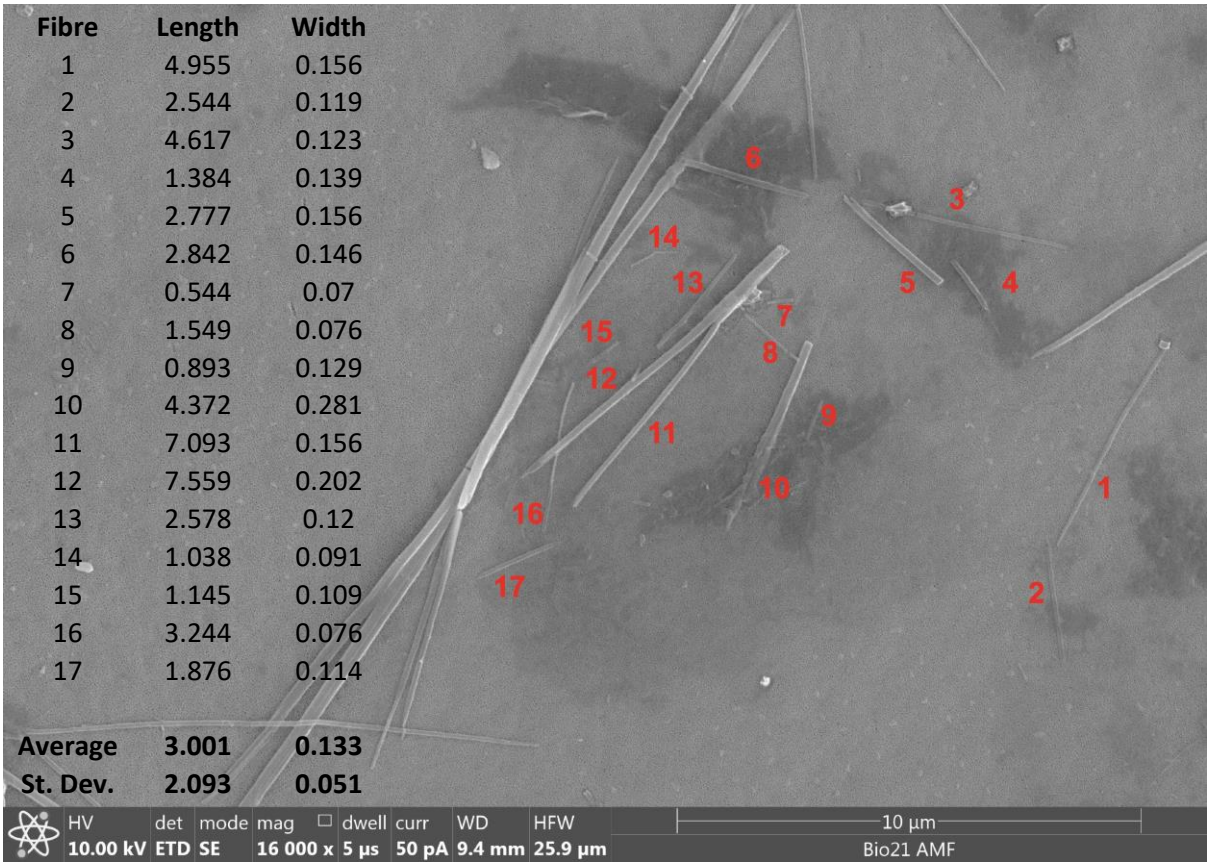

Fibre	Length	Width
1	4.955	0.156
2	2.544	0.119
3	4.617	0.123
4	1.384	0.139
5	2.777	0.156
6	2.842	0.146
7	0.544	0.07
8	1.549	0.076
9	0.893	0.129
10	4.372	0.281
11	7.093	0.156
12	7.559	0.202
13	2.578	0.12
14	1.038	0.091
15	1.145	0.109
16	3.244	0.076
17	1.876	0.114
Average	**3.001**	**0.133**
St. Dev.	**2.093**	**0.051**

Figure S2. A representative SEM image was selected and the fibres in the image were numbered and measured for length and width using ImageJ. The average length and width ± standard deviation were 3.00 ± 2.09 µm and 0.13 ± 0.05 µm, respectively. Measurement was only performed when the entire fibre was visible, therefore a small number of very large fibres were not included in the average and standard deviation calculations.

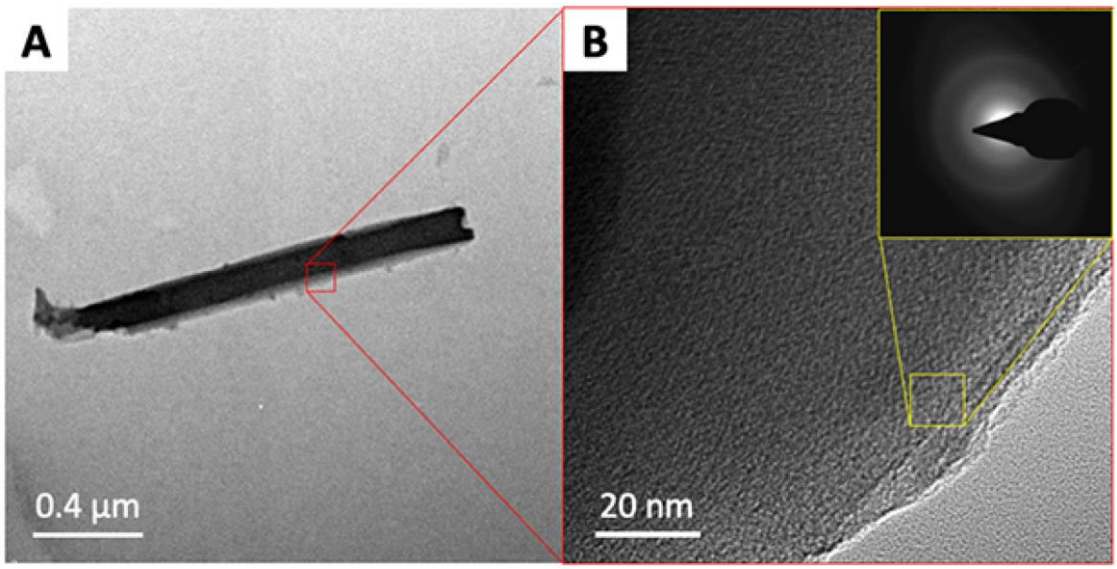

Figure S3. (A and B) High resolution TEM images of SA-TCPP. (B inset) Selected area electron diffraction (SAED) of the yellow box.

Author Manuscript

This article is protected by copyright. All rights reserved

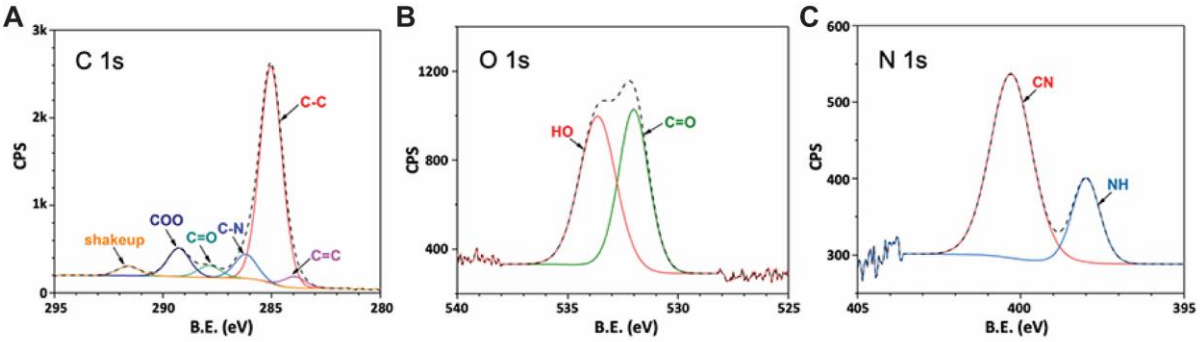

Figure S4. XPS spectra of (A) carbon 1s, (B) oxygen 1s, and (C) nitrogen 1s regions. Shakeup, COO, C=O, C-N, C-C, and C=C peaks were found at 292, 289, 288, 286, 285, and 284 eV, respectively. The C-C peak represented 71.7% of the area under the curve, with the remaining peaks representing 3.2-9.4% of the carbon 1s region. OH and C=O peaks were found at 532 and 534 eV and made up 47 and 52% of the area under the curve, consistent with the molecular structure of SA-TCPP. The nitrogen 1s region revealed peaks for C-N and N-H, binding energies of 400 and 398 eV, at a ratio of 3:1.

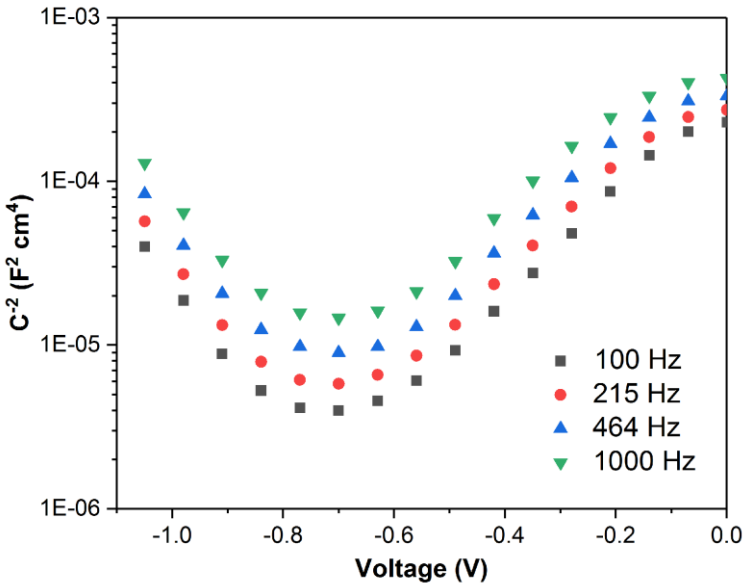

Figure S5. The Mott-Schottky plots of SA-TCPP. Four frequencies have been used to detect the flat band position of SA-TCPP semiconductor (-0.7 eV *vs.* SCE).

Author Manuscript

This article is protected by copyright. All rights reserved

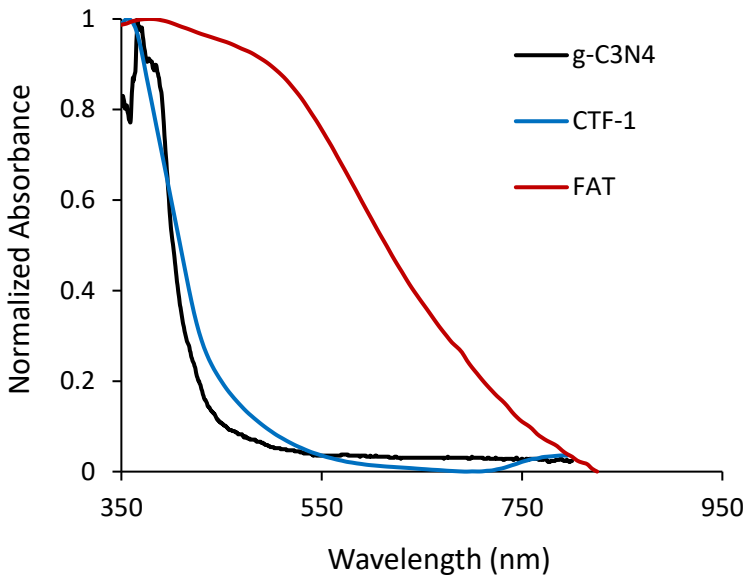

Figure S6. Normalized absorbance spectra of CTF-1, FAT, and g-C_3N_4 from 350 to 950 nm. Note: UV-Vis absorbance spectra were calculated from diffuse reflectance measurements taken in the solid state, and therefore should not be directly used as evidence suggesting photocatalytic ability under irradiation at a particular wavelength.

Author Manuscript

This article is protected by copyright. All rights reserved

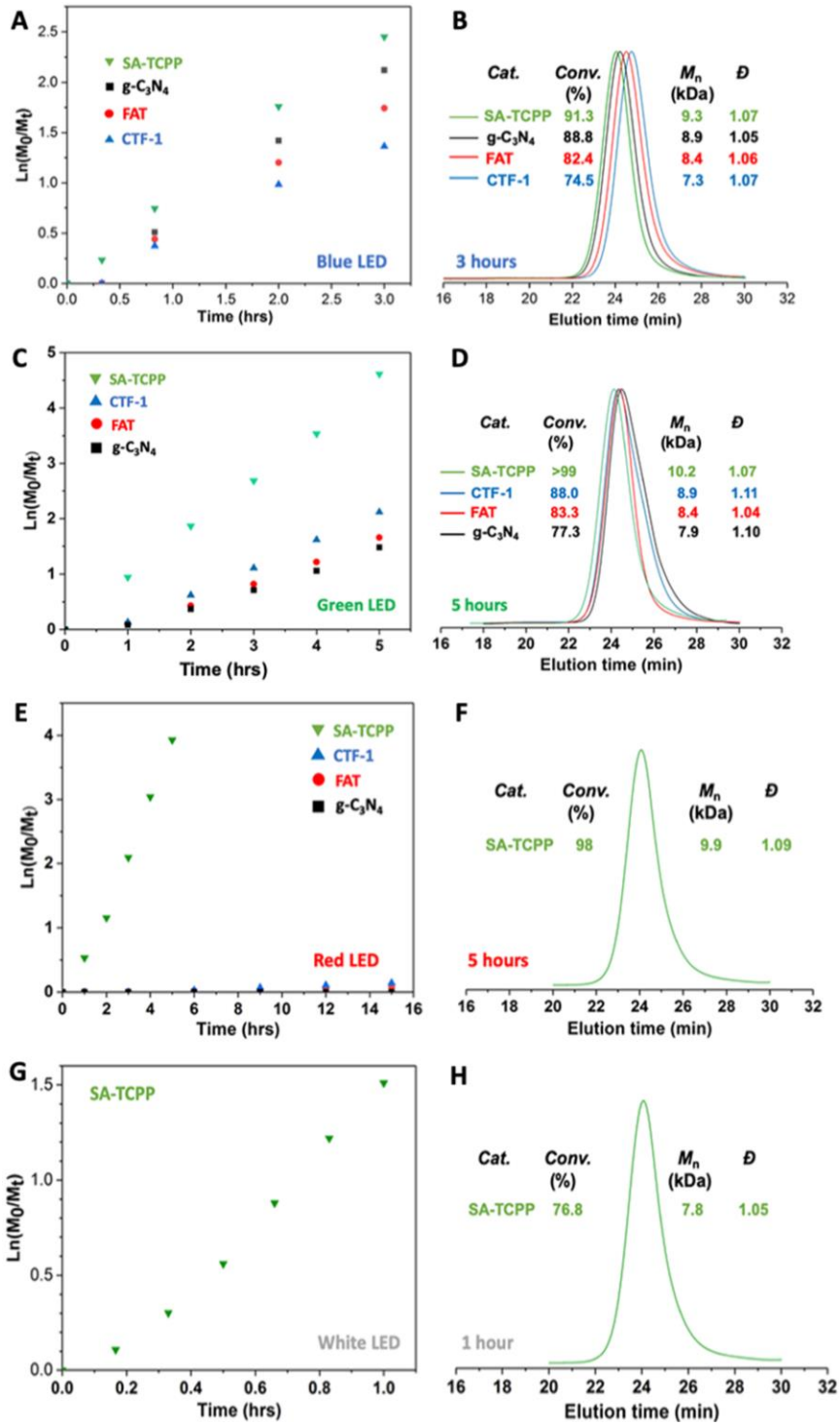

Figure S7. Polymerization kinetics and GPC traces from PET-RAFT polymerization of DMA in water with SA-TCPP, g-C3N4, FAT, and CTF-1 photocatalysts under blue (A and B), green (C and D), red (E and F), and white (G and H) LED light irradiation. All photocatalysts enabled PET-RAFT polymerization of DMA to reach high conversions under blue light irradiation, with SA-TCPP reaching 91% conversion in 3 hours. Under green light, >99% monomer conversion was observed in 5 hours using SA-TCPP, while the CTF-1, FAT, and g-C_3N_4 reached 88, 83, and 77% conversion, respectively. Only SA-TCPP resulting in polymer formation after 5 hours of irradiation. In all cases where polymers were formed, kinetics show linear semi-logarithmic plots of conversion versus irradiation time, indicating a constant radical concentration and controlled polymerization. All GPC traces were monomodal and symmetrical, with dispersities of 1.1 or below.

Author Manuscript

This article is protected by copyright. All rights reserved

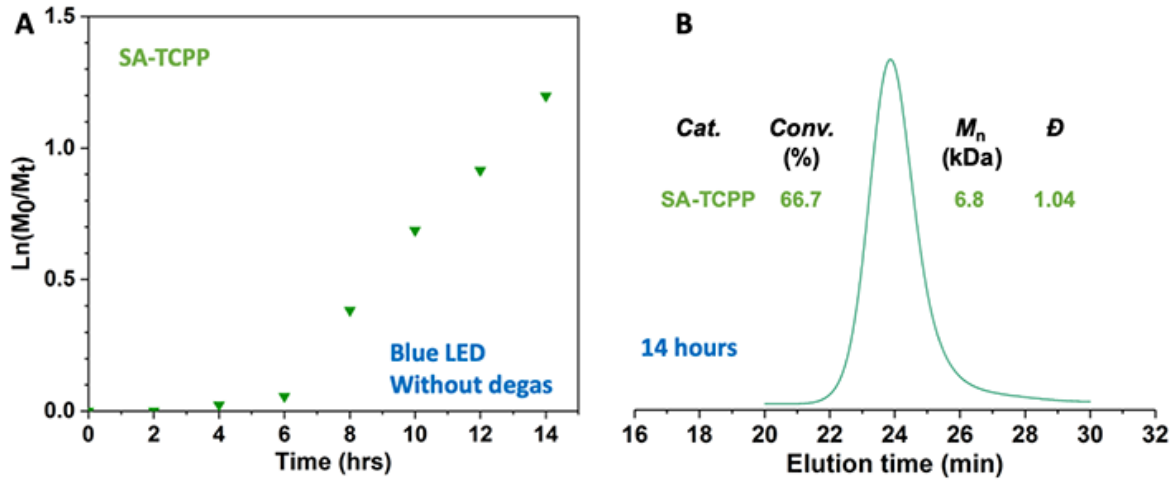

Figure S8. (A) Polymerization kinetics and (B) GPC trace of PET-RAFT polymerization of DMA in water under blue light without addition of TEOA or degassing. An induction period of nearly 6 hours was observed, with 67% conversion reached in 14 hours. GPC analysis showed a symmetrical, monomodal peak with a dispersity of 1.04.

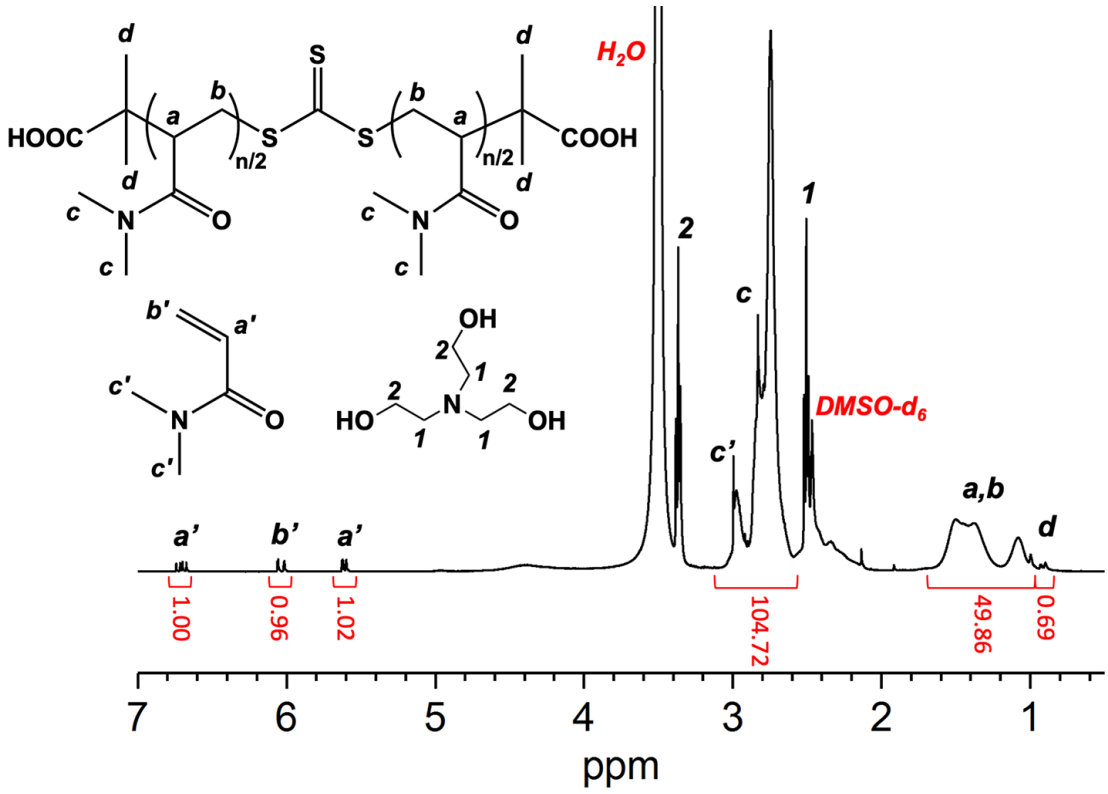

Figure S9. NMR spectrum of the final chain extension resulting in a pseudo-pentablock PDMA, with target DP 300. Integration of the RAFT agent methyl groups and polymer backbone indicate 289 DMA repeat units, corresponding to an M_n of 28.9 kDa. This result is in close agreement with the $M_{n,GPC}$ of 29.2 kDa, highlighting the "livingness" of the polymerization.

Author Manuscript

This article is protected by copyright. All rights reserved

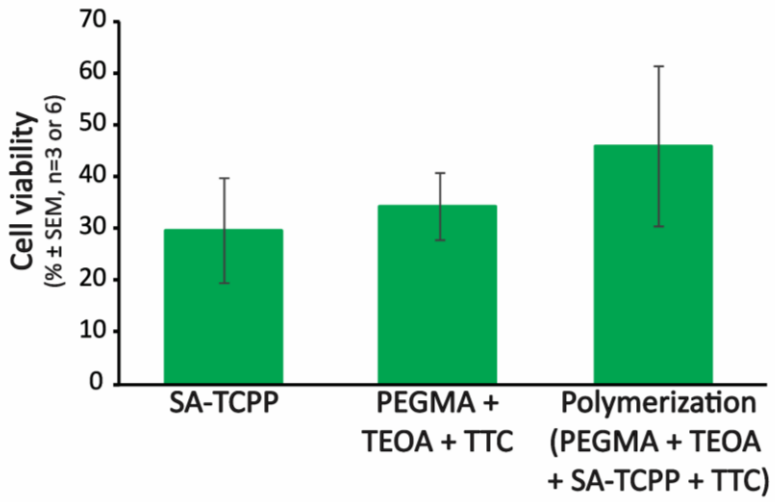

Figure S10. (B) Cell viability assay following red light irradiation for 45 minutes. Cells treated with SA-TCCP, PEGMA + TEOA + RAFT agent, or polymerization (SA-TCPP, PEGMA + TEOA + RAFT agent) in supplemented DMEM showed 30 ± 10 (n= 3), 34 ± 6.5 (n = 3), and 46 ± 15% (n = 6) cell viability ± standard error of the mean.

References

(1) Lai, J. T.; Filla, D.; Shea, R. Functional Polymers from Novel Carboxyl-Terminated Trithiocarbonates as Highly Efficient RAFT Agents. *Macromolecules* **2002,** *35* (18), 6754.

(2) Martin, D. J.; Qiu, K.; Shevlin, S. A.; Handoko, A. D.; Chen, X.; Guo, Z.; Tang, J. Highly efficient photocatalytic H2 evolution from water using visible light and structure-controlled graphitic carbon nitride. *Angew. Chem. Int. Ed.* **2014,** *53* (35), 9240.

(3) Wang, Y.; Bayazit, M. K.; Moniz, S. J. A.; Ruan, Q.; Lau, C. C.; Martsinovich, N.; Tang, J. Linker-controlled polymeric photocatalyst for highly efficient hydrogen evolution from water. *Energy & Environmental Science* **2017,** *10* (7), 1643.

(4) Xie, J.; Shevlin, S. A.; Ruan, Q.; Moniz, S. J. A.; Liu, Y.; Liu, X.; Li, Y.; Lau, C. C.; Guo, Z. X.; Tang, J. Efficient visible light-driven water oxidation and proton reduction by an ordered covalent triazine-based framework. *Energy & Environmental Science* **2018,** *11* (6), 1617.

(5) Wang, Y.; Silveri, F.; Bayazit, M. K.; Ruan, Q.; Li, Y.; Xie, J.; Catlow, C. R. A.; Tang, J. Bandgap engineering of organic semiconductors for highly efficient photocatalytic water splitting. *Adv. Energy Mater.* **2018,** *8* (24), 1801084.

Author Manuscript

This article is protected by copyright. All rights reserved